MITSUBISHI ELECTRIC RESEARCH LABORATORIES
http://www.merl.com

Ultra Wideband Impulse Radio Systems with Multiple Pulse Types

Sinan Gezici, Zafer Sahinoglu, Hisashi Kobayashi and Vincent Poor

TR2005-027   December 2005

Abstract

In an ultra wideband (UWB) impulse radio (IR) system, a number of pulses, each transmitted in an interval called a ̈frame ̧ is employed to represent one information symbol. Conventionally, a single type of UWB pulse is used in all frames of all users. In this paper, IR systems with multiple types of UWB pulses are considered, where different types of pulses can be used in different frames by different users. Both stored-reference (SR) and transmitted-reference (TR) systems are considered. First, the spectral properties of a multi-pulse IR system with polarity randomization is investigated. It is shown that the average power spectral density is the average of the spectral contents of different pulse shapes. Then, approximate closed-form expressions for the bit error probability of a multi-pulse SR-IR system are derived for RAKE receivers in asynchronous multiuser environments. The effects of both inter-frame interference (IFI) and multiple-access interference (MAI) are analyzed. The theoretical and simulation results indicate that SR-IR systems that are more robust against IFI and MAI than a ̈conventionalŠR-IR system can be designed with multiple types of ultra-wideband pulses. Finally, a multi-pulse TR-IR system is proposed, in which the transmitter and the receiver are designed in order to mitigate the effects of IFI and MAI. The performance of the proposed receiver is analyzed approximately and by simulations.

IEEE Journal on Select Areas in Communications

Ultra Wideband Impulse Radio Systems with Multiple Pulse Types[0]

Sinan Gezici[1,3], *Student Member, IEEE*, Zafer Sahinoglu[2], *Member, IEEE*,
Hisashi Kobayashi[1], *Life Fellow, IEEE*, and H. Vincent Poor[1], *Fellow, IEEE*

Abstract

In an ultra wideband (UWB) impulse radio (IR) system, a number of pulses, each transmitted in an interval called a "frame", is employed to represent one information symbol. Conventionally, a single type of UWB pulse is used in all frames of all users. In this paper, IR systems with multiple types of UWB pulses are considered, where different types of pulses can be used in different frames by different users. Both stored-reference (SR) and transmitted-reference (TR) systems are considered. First, the spectral properties of a multi-pulse IR system with polarity randomization is investigated. It is shown that the average power spectral density is the average of the spectral contents of different pulse shapes. Then, approximate closed-form expressions for the bit error probability of a multi-pulse SR-IR system are derived for RAKE receivers in asynchronous multiuser environments. The effects of both inter-frame interference (IFI) and multiple-access interference (MAI) are analyzed. The theoretical and simulation results indicate that SR-IR systems that are more robust against IFI and MAI than a "conventional" SR-IR system can be designed with multiple types of ultra-wideband pulses. Finally, a multi-pulse TR-IR system is proposed, in which the transmitter and the receiver are designed in order to mitigate the effects of IFI and MAI. The performance of the proposed receiver is analyzed approximately and by simulations.

Index Terms— Ultra-wideband (UWB), multi-pulse impulse radio (IR), stored-reference (SR), transmitted-reference (TR), performance analysis.

[0]This research is supported in part by the National Science Foundation under grant ANI-03-38807, and in part by the New Jersey Center for Wireless Telecommunications.

[1]Department of Electrical Engineering, Princeton University, Princeton, NJ 08544, USA, Tel: (609) 258-6868, Fax: (609)258-2158, email: sgezici@princeton.edu

[2]Mitsubishi Electric Research Labs, 201 Broadway, Cambridge, MA 02139, USA, e-mail: zafer@merl.com

[3]Corresponding author

I. INTRODUCTION

Since the US Federal Communications Commission (FCC) approved the limited use of ultra-wideband (UWB) technology [1], communications systems that employ UWB signals have drawn considerable attention. A UWB signal is defined to be one that possesses an absolute bandwidth larger than 500MHz or a relative bandwidth larger than 20% and can coexist with incumbent systems in the same frequency range due to its large spreading factor and low power spectral density. UWB technology holds great promise for a variety of applications such as short-range high-speed data transmission and precise location estimation.

Commonly, impulse radio (IR) systems, which transmit very short pulses with a low duty cycle, are employed to implement UWB systems ([2]-[7]). In an IR system, a number N_f of pulses are transmitted per symbol, and information is usually carried by the polarity of the pulses in a coherent system, or by the difference in the polarity of the pulses in a differentially-modulated system. In the former case, it is assumed that received pulse structure is known at the receiver and channel estimation can be performed; hence, RAKE receivers can be used to collect energy from different multipath components. Since the incoming signal structure is correlated by a locally stored reference (template) signal in this case, such a system is called a *stored-reference* (SR) system [8]. In the latter case, out of the N_f pulses transmitted per information symbol, half of them are used as reference pulses, whereas the remaining half are used as data pulses. The relative polarity of the reference and the data pulses carries the information. Since the reference pulses to be used in the demodulation are transmitted to the receiver, such a system is called a *transmitted-reference* (TR) system [7]. In a TR system, there is no need for channel estimation since the reference and the data pulses are effected by the same channel, assuming that the channel is constant for a sufficiently long time interval, which is usually the case for UWB systems. On the other hand, a lower throughput is expected since half of the energy is used for non-information carrying pulses. Also since the transmitted reference is used as a noisy template at the receiver, more effective noise terms are generated.

Considering a conventional SR-IR system, a single type of UWB pulse is transmitted in all frames of all users [2]. In asynchronous multiuser environments, the autocorrelation function of the pulse becomes an important factor in determining the effects of inter-frame interference (IFI) and multiple-access interference (MAI) [9]. In order to reduce those effects, UWB pulses with fast decaying autocorrelation functions are desirable. However, such an autocorrelation function also results in a considerable decrease in the desired signal part of the receiver output in the presence of timing jitter [10]. Moreover, when there is an exact overlap between a pulse and an interfering pulse, the interference is usually very significant. Hence, there is not much flexibility in choosing the pulse shape in order to combat against interference effects. However, in SR-IR systems with multiple types of UWB pulses, the effects of interference can be mitigated by using different types of UWB pulses with good cross-correlation properties. Multi-pulse SR-IR systems have recently been proposed in [11]. However, there has been no theoretical analysis of such systems, in terms of their spectral properties and bit error probability (BEP) performance, and no quantitative investigation of the gains that can be obtained by multiple types of UWB pulses. In this paper, we consider this problem in an asynchronous multiuser environment and analyze the BEP performance of a generic RAKE receiver over frequency-selective channels. The results are valid for arbitrary numbers of UWB pulse types, and hence cover the single-pulse system as a special case.

Moreover, considering TR-IR systems, we propose a multi-pulse transmitter and receiver structure, which is the first application of the multi-pulse approach to TR-IR systems. The proposed scheme aims to mitigate the IFI and MAI by appropriate design of a signalling structure. The performance of the proposed system is analyzed approximately, and simulation results are presented.

In addition to the performance analysis of the multi-pulse IR systems, the average power spectral density (PSD) of a generic multi-pulse IR signal is derived and a simple relationship between the Fourier transforms of the UWB pulses and the average PSD of the transmitted signal is obtained.

The remainder of the paper is organized as follows. Section II describes a generic transmitted signal model, which reduces to SR- and TR-IR systems as special cases. Then, Section III analyzes the spectral properties of this generic IR signal structure. After describing the received signal in Section IV, the performance of multi-pulse SR-IR systems employing RAKE receivers is analyzed in Section V. Section VI proposes a multi-pulse TR-IR system, and presents an approximate performance analysis. The simulation results are given in Section VII, which is followed by the concluding remarks in Section VIII.

II. Transmitted Signal Model

The transmitted signal from the kth user in a multi-pulse UWB-IR system can be expressed as

$$s^{(k)}(t) = \frac{1}{\sqrt{N_f}} \sum_{i=-\infty}^{\infty} \sum_{n=0}^{N_p-1} s_{i,n}^{(k)}(t), \tag{1}$$

where N_f is the number of pulses transmitted per information symbol, N_p is the number of different pulse types, and $s_{i,n}^{(k)}(t)$ represents the UWB pulses of type n transmitted for the ith information symbol of user k. Note that the signal model in (1) can also represent cases in which the number of pulse types is less than N_p, by using the same pulses for different pulse indices. Also different users can have different ordering of the pulses in one period, which can be useful for reducing the effects of MAI. The number of pulses per symbol, N_f, is assumed to be an even multiple of N_p for simplicity of notation and $s_{i,n}^{(k)}(t)$ is expressed as follows:

$$s_{i,n}^{(k)}(t) = \sum_{j=iN_f/(2N_p)}^{(i+1)\frac{N_f}{2N_p}-1} \Big\{ b_{1,j}^{(k)}\, d_{2jN_p+n}^{(k)}\, p_n^{(k)}\left(t-(2jN_p+n)T_f - c_{2jN_p+n}^{(k)}T_c\right) + b_{2,j}^{(k)}\, d_{(2j+1)N_p+n}^{(k)}\, p_n^{(k)}\left(t-(2jN_p+n)T_f - T_n^{(k)} - c_{(2j+1)N_p+n}^{(k)}T_c\right)\Big\}. \tag{2}$$

In (2), $p_n^{(k)}(t)$ is the UWB pulse of type n for user k, T_f is the frame interval, T_c is the chip interval, and $T_n^{(k)}$ is the distance between the two pulses in a pair of type n for the kth user, considering the pulses from a given type being grouped into pairs as shown in Figure 1. The time-hopping (TH) code for user k is denoted by $c_j^{(k)}$, which is an integer taking values in the set $\{0, 1, \ldots, N_c - 1\}$, with N_c being the number of chips per frame, which prevents catastrophic collisions between different users. The polarity, or the spreading, code, $d_j^{(k)} \in \{-1, +1\}$, changes the polarity of the pulses, which smoothes the power spectral density of the transmitted signal [12] and provides robustness against MAI [13]. The information is represented by $b_{1,j}^{(k)}$ and $b_{2,j}^{(k)}$, which carry the same information for an SR system, and carry the information in the difference between their values for a TR system.

The general signal model in (2) can represent SR and TR systems as special cases:

A. Stored Reference Impulse Radio

For the SR system, $b_{1,j}^{(k)} = b_{2,j}^{(k)} = b_{\lfloor 2N_pj/N_f \rfloor}^{(k)}$, $T_n^{(k)} = N_pT_f \ \forall n, k$, and each frame has independent time-hopping and polarity codes.

B. Transmitted Reference Impulse Radio

For the TR system, $b_{1,j}^{(k)} = 1$ and $b_{2,j}^{(k)} = b_{\lfloor 2N_pj/N_f \rfloor}^{(k)}$. In other words, the first pulse in (2) is the reference pulse and the second one is the data pulse. As shown in Figure 1, this results in a structure in which the first N_p pulses are the reference pulses, the next N_p pulses are the data pulses, and which follows this alternating structure.

Note that $T_n^{(k)}$ can be chosen to be larger than N_pT_f for the TR system if the TH sequence is constrained to a set $\{0,1,\ldots,N_h-1\}$ with $N_h<N_c$. In this case, different values from the set $[N_pT_f,(N_p+1)T_f-N_hT_c]$ can be chosen for different users and/or different pulse types in order to provide extra robustness against the effects of interference.

Also each reference-data pulse pair has the same TH and polarity codes in order to facilitate simple delay and multiplication operation. In other words, $d^{(k)}_{2jN_p+n}=d^{(k)}_{(2j+1)N_p+n}$, and $c^{(k)}_{2jN_p+n}=c^{(k)}_{(2j+1)N_p+n}$, for $j=iN_f/(2N_p),\ldots,(i+1)N_f/(2N_p)-1$, $\forall\ i$, $n=0,1,\ldots,N_p-1$.

III. Power Spectrum Density of Multi-pulse UWB-IR Systems

In order to evaluate the spectral properties of the transmitted signal, the (average) power spectral density of the signal must be calculated. Therefore, we first calculate the autocorrelation function of $s(t)$ as follows[4]:

$$\phi_{ss}(t+\tau,t)=\mathrm{E}\{s(t+\tau)s(t)\}=\frac{1}{N_f}\sum_{i=-\infty}^{\infty}\sum_{n=0}^{N_p-1}\mathrm{E}\{s_{i,n}(t+\tau)s_{i,n}(t)\},\tag{3}$$

where we employ the fact that the polarity codes are i.i.d. for different bit and pulse indices.

From (2), $\mathrm{E}\{s_{i,n}(t+\tau)s_{i,n}(t)\}$ can be calculated as (see Appendix A)

$$\begin{aligned}\mathrm{E}\{s_{i,n}(t+\tau)s_{i,n}(t)\}=\sum_{j=iN_f/N_p}^{(i+1)N_f/N_p-1}&\mathrm{E}\{p_n(t+\tau-(jN_p+n)T_f-c_{jN_p+n}T_c)\\&\times p_n(t-(jN_p+n)T_f-c_{jN_p+n}T_c)\}.\end{aligned}\tag{4}$$

From (3) and (4), it is observed that $s(t)$ is not wide-sense stationary (WSS) since the autocorrelation function is not independent of t. However, note that $s(t)$ is a zero mean cyclostationary process since $\phi_{ss}(t+\tau,t)$ is periodic with a period of N_pT_f [14]. Therefore, we can obtain the time-average autocorrelation function as

$$\bar{\phi}_{ss}(\tau)=\frac{1}{N_pT_f}\int_0^{N_pT_f}\phi_{ss}(t+\tau,t)dt=\frac{1}{N_pT_fN_f}\sum_{n=0}^{N_p-1}\int_{-\infty}^{\infty}p_n(t+\tau)p_n(t)dt,\tag{5}$$

[4]We drop the user index k in this section, for notational convenience.

the Fourier transform of which gives the average PSD as follows:

$$\Phi_{ss}(f) = \frac{1}{N_p T_s} \sum_{n=0}^{N_p-1} |W_n(f)|^2, \tag{6}$$

where $W_n(f)$ is the Fourier transform of $p_n(t)$.

Note from (6) that the average PSD of the signal is the average value of the squares of the Fourier transforms of the pulses. The dependence on the pulse spectra only is a consequence of the pulse-based polarity randomization, as considered for impulse radio systems in [12] and [15]. Moreover, we note that the multi-pulse system can have more flexibility in shaping the PSD by proper choice of the UWB pulses.

IV. Channel Model and Received Signal

We consider the following channel model for user k:

$$h^{(k)}(t) = \sum_{l=0}^{L-1} \alpha_l^{(k)} \delta(t - \tau_l^{(k)}), \tag{7}$$

where $\alpha_l^{(k)}$ and $\tau_l^{(k)}$ are, respectively, the fading coefficient and the delay of the lth path for user k.

Using the channel model in (7) and the transmitted signal in (1), the received signal can be expressed as

$$\begin{aligned} r(t) = \sum_{k=1}^{K} \sqrt{\frac{E_k}{N_f}} \sum_{i=-\infty}^{\infty} \sum_{n=0}^{N_p-1} \sum_{j=iN_f/(2N_p)}^{(i+1)\frac{N_f}{2N_p}-1} \{ & b_{1,j}^{(k)}\, d_{2jN_p+n}^{(k)}\, u_n^{(k)} \left(t - (2jN_p + n)T_f - c_{2jN_p+n}^{(k)} T_c - \tau_0^{(k)}\right) \\ & + b_{2,j}^{(k)}\, d_{(2j+1)N_p+n}^{(k)}\, u_n^{(k)} \left(t - (2jN_p + n)T_f - T_n^{(k)} - c_{(2j+1)N_p+n}^{(k)} T_c - \tau_0^{(k)}\right) \} + \sigma n(t), \end{aligned} \tag{8}$$

with

$$u_n^{(k)}(t) = \sum_{l=0}^{L-1} \alpha_l^{(k)} w_n^{(k)}(t - \tau_l^{(k)} + \tau_0^{(k)}), \tag{9}$$

where $w_n^{(k)}(t)$ is the received UWB pulse of type n for user k, E_k determines the received energy from user k, and $n(t)$ is a zero mean white Gaussian process with unit spectral density.

V. ANALYSIS OF RAKE RECEIVERS FOR MULTI-PULSE SR-IR

Since $b_{1,j}^{(k)} = b_{2,j}^{(k)} = b_{\lfloor 2N_p j/N_f \rfloor}^{(k)}$, and each frame has independent time-hopping and polarity codes for the SR-IR system, the received signal in (8) can be expressed, after some manipulation, as

$$r(t) = \sum_{k=1}^{K} \sqrt{\frac{E_k}{N_f}} \sum_{j=-\infty}^{\infty} b_{\lfloor j/N_f \rfloor}^{(k)} \, d_j^{(k)} \, u_j^{(k)} \left(t - jT_f - c_j^{(k)} T_c - \tau_0^{(k)} \right) + \sigma n(t), \tag{10}$$

with $u_j^{(k)}(t)$ given by (9). For the indices of the pulse types, such as in (9), the *modulo* N_p operation is implicitly assumed. In other words, for any $n \in \{0, 1, \ldots, N_p - 1\}$, $w_n(t) = w_{n+kN_p}(t)$ for all integers k.

We consider a generic RAKE receiver that can represent different combining schemes, such as equal gain or maximal ratio combining. It can be expressed as the correlation of the received signal in (8) with the following template signal, where we consider the 0th bit of user 1 without loss of generality:

$$s_{\text{temp}}^{(1)}(t) = \sum_{j=0}^{N_f - 1} d_j^{(1)} v_j^{(1)} (t - jT_f - c_j^{(1)} T_c), \tag{11}$$

with

$$v_j^{(1)}(t) = \sum_{l=0}^{L-1} \beta_l w_j^{(1)} (t - \tau_l^{(1)}), \tag{12}$$

where β_l denotes the RAKE combining coefficient for the lth path. We assume that $\tau_0^{(1)} = 0$, and $\tau_0^{(k)} \in [0, N_f T_f)$, for $k = 2, \ldots, K$, again without loss of generality. Note that for a partial or selective RAKE receiver [16], the combining coefficients for those paths that are not used are set to zero.

We assume that the delay spreads of the channels are not larger than one frame interval; that is $\tau_{L-1}^{(k)} \leq T_f$, $\forall k$. In other words, the frame interval is chosen to be sufficiently large so that the pulses in one frame can interfere only with those in the adjacent frames.

Using (10) and (11), the decision variable for detecting the 0th bit of user 1 can be obtained as:

$$Y = \int r(t) s_{\text{temp}}^{(1)}(t) dt = b_0^{(1)} \sqrt{\frac{E_1}{N_f}} \sum_{j=0}^{N_f - 1} \phi_{u_j^{(1)} v_j^{(1)}}(0) + I + M + N, \tag{13}$$

with

$$\phi_{u_i^{(k)} v_j^{(l)}}(x) = \int u_i^{(k)}(t - x) v_j^{(l)}(t) dt, \tag{14}$$

where the first term in (13) is the desired signal part of the output, I is the IFI, M is the MAI, and N is the output noise. For simplicity of notation, bit indices are not shown.

A. Inter-frame Interference

The IFI occurs when a pulse of the desired user, user 1, in a given frame spills over to an adjacent frame due to multipath and consequently interferes with the pulse in that frame. The IFI for the 0th symbol can be expressed, using (10), (11) and (14), as the sum of the IFI to each frame of the template signal:

$$I = \sqrt{\frac{E_1}{N_f}} \sum_{j=0}^{N_f-1} \hat{I}_j, \tag{15}$$

where

$$\hat{I}_j = d_j^{(1)} \sum_{\substack{m=-\infty \\ m\neq j}}^{\infty} d_m^{(1)} b_{\lfloor m/N_f \rfloor}^{(1)} \phi_{u_m^{(1)} v_j^{(1)}} \left((m-j)T_f + (c_m^{(1)} - c_j^{(1)})T_c \right). \tag{16}$$

Due to the assumption on the delay spreads of the channels, the IFI occurs only between adjacent frames. Hence, $\hat{I}_j$ in (16) becomes

$$\hat{I}_j = d_j^{(1)} \sum_{m\in\{-1,+1\}} d_{j+m}^{(1)} b_{\lfloor (j+m)/N_f \rfloor}^{(1)} \phi_{u_{j+m}^{(1)} v_j^{(1)}} \left(mT_f + (c_{j+m}^{(1)} - c_j^{(1)})T_c \right). \tag{17}$$

Let $N_f = N_r N_p$. Then, we can re-express (15) as

$$I = \sqrt{\frac{E_1}{N_r}} \sum_{j=0}^{N_r-1} \tilde{I}_j, \tag{18}$$

where $\tilde{I}_j = \frac{1}{\sqrt{N_p}} \sum_{n=0}^{N_p-1} \hat{I}_{jN_p+n}$ with $\hat{I}_j$ being given by (17). In Appendix B, we show that $\{\tilde{I}_j\}_{j=0}^{N_r-1}$ forms a 1-dependent sequence[5], and hence we approximate the distribution of the IFI term in (17) using a central limit argument for dependent sequences [30].

Proposition 5.1: Consider a random TH SR-IR system with pulse-based polarity randomization, which employs $N_p > 1$ different UWB pulses. Then, the IFI at the output of the RAKE receiver, expressed by (13), is asymptotically distributed as follows

$$I \sim \mathcal{N}\left(0\,,\, \frac{E_1}{N_p N_c^2} \sum_{n=0}^{N_p-1} \left[\sigma^2_{\mathrm{IFI},1}(n) + 2\sigma^2_{\mathrm{IFI},2}(n)\right]\right), \tag{19}$$

[5]A sequence $\{X_n\}_{n\in\mathbb{Z}}$ is called a D-dependent sequence, if all finite dimensional marginals $(X_{n_1}, ..., X_{n_i})$ and $(X_{m_1}, ..., X_{m_j})$ are independent whenever $m_1 - n_i > D$.

as $\frac{N_f}{N_p} \longrightarrow \infty$, where

$$\sigma^2_{\mathrm{IFI},1}(n) = \sum_{l=1}^{N_c} l \, \left(\phi^2_{u^{(1)}_{n+1} v^{(1)}_n}(lT_c) + \phi^2_{u^{(1)}_{n-1} v^{(1)}_n}(-lT_c) \right), \tag{20}$$

and

$$\sigma^2_{\mathrm{IFI},2}(n) = \sum_{l=1}^{N_c} l \, \phi_{u^{(1)}_{n+1} v^{(1)}_n}(lT_c) \phi_{u^{(1)}_n v^{(1)}_{n+1}}(-lT_c). \tag{21}$$

Proof: See Appendix B.

Due to the FCCs regulation on peak to average ratio (PAR), N_f cannot be chosen very small in practice. Since we transmit a certain amount of energy in a constant symbol interval, as N_f gets smaller, the signal becomes peakier as shown in Figure 2. Therefore, the approximation for large N_f/N_p can be quite accurate for real systems depending on the number of pulse types and the other system parameters.

From Proposition 5.1, the following result for a double-pulse system can be obtained.

Corollary 5.1: Consider a random TH SR-IR system with pulse-based polarity randomization, where the UWB pulses $w_0(t)$ and $w_1(t)$, which are both even functions, are transmitted alternately. For this system, the IFI in (13) is approximately distributed as follows for large N_f:

$$I \sim \mathcal{N}\left(0\,,\, \frac{E_1}{N_c^2} \sum_{l=1}^{N_c} l \, \left[\phi_{u^{(1)}_0 v^{(1)}_1}(-lT_c) + \phi_{u^{(1)}_0 v^{(1)}_1}(lT_c) \right]^2 \right). \tag{22}$$

The distribution of the IFI for the case where a single UWB pulse $w_0(t)$ is used in all the frames is given by [17]

$$I \sim \mathcal{N}\left(0\,,\, \frac{E_1}{N_c^2} \sum_{l=1}^{N_c} l \, \left[\phi_{u^{(1)}_0 v^{(1)}_0}(-lT_c) + \phi_{u^{(1)}_0 v^{(1)}_0}(lT_c) \right]^2 \right). \tag{23}$$

Note that in an IFI-limited scenario, the autocorrelation function of the UWB pulse is the determining factor for a single-pulse system. However, for the system using multiple types of UWB pulses, the IFI is determined by the cross-correlations of different pulses. Note that it is possible to design the pulses so that they are orthogonal and their cross-correlations decay quickly, e.g. modified Hermite pulses (MHPs) [18]. However, the autocorrelation function always causes large values when there is an exact overlap of the multipath components. Also a rapidly decaying autocorrelation function, which is good for combatting the IFI, may not be very desirable since small timing jitter in the system could result in a significant loss in the desired signal part of the decision variable. Therefore, the multi-pulse IR system is expected to have better IFI rejection capability than the single-pulse system. For example, for a system with $N_f = 20$,

$N_c = 30$ and $L = 20$, the power of the IFI is reduced by about $\%30$ by using the 4th and 5th order MHPs instead of using the 4th order MHP only.

B. Multiple-Access Interference

Consider the MAI term M in (13), which is the sum of the interference terms from $(K-1)$ users

$$M = \sum_{k=2}^{K} M^{(k)}, \tag{24}$$

where $M^{(k)}$ can be expressed as

$$M^{(k)} = \sqrt{\frac{E_k}{N_f}} \sum_{j=0}^{N_f-1} \hat{M}_j^{(k)}, \tag{25}$$

with $\hat{M}_j^{(k)}$ denoting the MAI from user k to the jth frame of the first user. From (10), (11) and (14), $\hat{M}_j^{(k)}$ can be expressed as

$$\hat{M}_j^{(k)} = d_j^{(1)} \sum_{m=-\infty}^{\infty} d_m^{(k)} b_{\lfloor m/N_f \rfloor}^{(k)} \phi_{u_m^{(k)} v_j^{(1)}} \left((m-j)T_f + (c_m^{(k)} - c_j^{(1)})T_c + \tau_0^{(k)} \right), \tag{26}$$

where $\tau_0^{(k)}$ denotes the amount of asynchronism between user k and the user of interest, user 1, since we assume $\tau_0^{(1)} = 0$.

For a given value of $\tau_0^{(k)}$, the distribution of the MAI from user k can be obtained approximately from the following proposition:

Proposition 5.2: Consider a random TH SR-IR system with pulse-based polarity randomization, which employs N_p different types of UWB pulses. Then, the MAI from user k, $M^{(k)}$ in (25), given $\tau_0^{(k)}$, is asymptotically distributed as follows

$$M^{(k)} | \tau_0^{(k)} \sim \mathcal{N}\left(0\,,\, \frac{E_k}{N_p N_c^2} \sum_{n=0}^{N_p-1} \sigma^2_{\mathrm{MAI},k}(n, \tau_0^{(k)})\right), \tag{27}$$

as $\frac{N_f}{N_p} \longrightarrow \infty$, where

$$\sigma^2_{\mathrm{MAI},k}(n, \tau_0^{(k)}) = \sum_{m \in \mathcal{A}} \sum_{l=-(N_c-1)}^{N_c-1} (N_c - |l|)\, \phi^2_{u_m^{(k)} v_n^{(1)}} \left(((m-n)N_c + l)\, T_c + \tau_0^{(k)} \right), \tag{28}$$

with $\mathcal{A} = \left\{ \left\lceil n - 2 + 1/N_c - \tau_0^{(k)}/T_f \right\rceil, \ldots, \left\lfloor n + 2 - 1/N_c - \tau_0^{(k)}/T_f \right\rfloor \right\}$.

Proof: See Appendix C.

Note that the Gaussian approximation in Proposition 5.2 is different from the standard Gaussian approximation (SGA) used in analyzing a system with many users ([27]-[29]). Proposition 5.2 states that when the number of *pulses* per information symbol is large compared to the number of different pulse types, the MAI from an interfering user is approximately distributed as a Gaussian random variable. This idea is similar to the improved Gaussian approximation approach in [19], where the large processing gain of a CDMA system leads to normally distributed MAI conditioned on some systems parameters.

Denote the amount of asynchronism between user k and user 1 as $\tau_0^{(k)} = \lfloor \tau_0^{(k)}/T_c \rfloor T_c + \epsilon_k$, where $\epsilon_k \in [0, T_c)$. When a single type of UWB pulse is employed in the system, it can be shown from Proposition 5.2 that the distribution of $M^{(k)}$ is given by the following result:

Corollary 5.2: Consider a random TH SR-IR system with pulse-based polarity randomization, where the UWB pulse $w_0(t)$ is employed in all frames of all users. Then, the conditional distribution of the MAI from user k is given by

$$M^{(k)} | \tau_0^{(k)} \sim \mathcal{N}\left(0\,,\, \frac{E_k}{N_c} \sum_{l=-N_c}^{N_c-1} \phi^2_{u_0^{(k)} v_0^{(1)}}(lT_c + \epsilon_k)\right). \tag{29}$$

Note from Corollary 5.2 that the distribution of $M^{(k)}$ depends on ϵ_k, instead of $\tau_0^{(k)}$, for a single-pulse system. This is because the probability that a given pulse of the desired user collides with the pulses of user k is the same for all delays $\tau_0^{(k)}$ with identical ϵ_k values, due to the random TH codes, and the same amount of average interference occurs when the same pulses are used in all frames.

Denote $\boldsymbol{\tau} = [\tau_0^{(2)} \cdots \tau_0^{(K)}]$. Then, given $\boldsymbol{\tau}$, the distribution of the total MAI M in (13) can be approximated by

$$M | \boldsymbol{\tau} \sim \mathcal{N}\left(0\,,\, \frac{1}{N_p N_c^2} \sum_{k=2}^{K} \sum_{n=0}^{N_p-1} E_k\, \sigma^2_{\mathrm{MAI},k}(n, \tau_0^{(k)})\right), \tag{30}$$

for large N_f/N_p, where $\sigma^2_{\mathrm{MAI},k}(n, \tau_0^{(k)})$ is as in (28). Note that it is not necessary to have a large number of users, or equal energy interferers (perfect power control), for the expression in (30) to be accurate. The only requirement is to have a large ratio between the number of pulses per symbol and the number of pulse types.

When the delays of the interferers are unknown and/or an average performance measure is to be obtained, then each interferer is assumed to have a uniformly distributed delay with respect to the desired user; that is, $\tau_0^{(k)} \sim [0, N_f T_f)$, $\forall k$. In this case, the performance measure, such as the BEP expression, needs to be averaged over the distribution of $\boldsymbol{\tau}$.

C. Output Noise

The output noise N in (13) is distributed as $\mathcal{N}\left(0\,,\,\sigma^2\int|s_{\text{temp}}^{(1)}(t)|^2dt\right)$. Using the expression in (11) for $s_{\text{temp}}^{(1)}(t)$, we can approximate the distribution of N for an SR-IR system with a single UWB pulse $w_0(t)$ as $N\sim\mathcal{N}\left(0\,,\,N_f\sigma^2\phi_{v_0^{(1)}}(0)\right)$, for large values of N_f, where $\phi_{v_j^{(k)}}(x)=\int v_j^{(k)}(t-x)v_j^{(k)}(t)dt$ is the autocorrelation function of $v_j^{(k)}(t)$.

Similarly, for an SR-IR system employing N_p types of pulses, we obtain the approximate distribution of N as $N\sim\mathcal{N}\left(0\,,\,\sigma^2\frac{N_f}{N_p}\sum_{n=0}^{N_p-1}\phi_{v_n^{(1)}}(0)\right)$, for large N_f/N_p.

D. Bit Error Probability

Using the results in the previous sections, we can obtain an approximate BEP expression for the multi-pulse SR-IR system as follows:

$$P_e(\boldsymbol{\tau})\approx Q\left(\frac{\sqrt{\frac{E_1}{N_p}}\sum_{n=0}^{N_p-1}\phi_{u_n^{(1)}v_n^{(1)}}(0)}{\sqrt{\sum_{n=0}^{N_p-1}\left\{\frac{E_1}{N_cN}[\sigma^2_{\text{IFI},1}(n)+2\sigma^2_{\text{IFI},2}(n)]+\frac{1}{N_cN}\sum_{k=2}^{K}E_k\sigma^2_{\text{MAI},k}(n,\tau_0^{(k)})+\sigma^2\phi_{v_n^{(1)}}(0)\right\}}}\right), \tag{31}$$

for large N_f/N_p, where $\boldsymbol{\tau}=[\tau_0^{(2)}\cdots\tau_0^{(K)}]$, $N=N_cN_f$ is the total processing gain of the system, and $\sigma^2_{\text{IFI},1}(n)$, $\sigma^2_{\text{IFI},1}(n)$ and $\sigma^2_{\text{MAI},k}(n,\tau_0^{(k)})$ are as in (20), (21) and (28), respectively.

If we consider a synchronous scenario, where $\tau_0^{(k)}=0$, for $k=1,2,\ldots,K$, then the unconditional BEP is given by $P_e^{\text{sync}}=P_e(\mathbf{0})$, with $P_e(\boldsymbol{\tau})$ being given by (31).

For an asynchronous system, we assume that $\tau_0^{(2)},\ldots,\tau_0^{(K)}$ are i.i.d. distributed as $\mathcal{U}[0,T_s)$, where $T_s=N_fT_f$ is the symbol interval. Hence, the unconditional BEP can be obtained by

$$P_e^{\text{async}}=\frac{1}{T_s^{K-1}}\int_0^{T_s}\cdots\int_0^{T_s}P_e(\boldsymbol{\tau})d\tau_0^{(2)}\ldots d\tau_0^{(K)}. \tag{32}$$

Due to the periodicity of the pulse structure, we can show that it is enough to average over an interval of length N_pT_f instead of N_fT_f. Hence, P_e^{async} can be expressed as

$$P_e^{\text{async}}=\frac{1}{(N_pT_f)^{K-1}}\int_0^{N_pT_f}\cdots\int_0^{N_pT_f}P_e(\boldsymbol{\tau})d\tau_0^{(2)}\ldots d\tau_0^{(K)}. \tag{33}$$

In order to calculate P_e^{async}, numerical techniques or Monte-Carlo simulations can be used. For example, by generating N_m vectors according to the uniform distribution in $[0, N_pT_f)^{K-1}$, we can approximate P_e^{async} by Monte-Carlo simulations as

$$P_e^{\text{async}} = \frac{1}{N_m}\sum_{i=1}^{N_m} P_e(\boldsymbol{\tau}_i), \tag{34}$$

where $\boldsymbol{\tau}_i$ denotes the ith random vector of interferer delays.

Note that the BEP expression in (33) becomes more accurate as N_f/N_p gets larger, without the need for large number of users or equal energy interferers, which are needed for accurate BEP using the SGA. The SGA directly calculates the average value of the variance of the total MAI instead of averaging over a conditional BEP expression in (31). In other words, P_e^{async} is approximated by the expression in (31) with the only change of using $\frac{1}{N_pT_f}\int_0^{N_pT_f}\sigma^2_{\text{MAI},k}(n,\tau_0^{(k)})d\tau_0^{(k)}$ instead of $\sigma^2_{\text{MAI},k}(n,\tau_0^{(k)})$. Of course, this expression is easier to evaluate than the expression in (33), especially when there is a large number of users. Therefore, in such a case, the SGA might be preferred if the users' power levels are not very different. But for systems with small numbers of interferers, such as an IEEE 802.15.3a personal area network (PAN), the expression in (33) is not very difficult to evaluate and can result in more accurate BEP evaluations.

Now consider the case in which a single type of UWB pulse $w_0(t)$ is employed for all users. The BEP expression for this scenario can be obtained from (13), (23), (29), and Section V-C as

$$P_e(\boldsymbol{\epsilon}) \approx Q\left(\frac{\sqrt{E_1}\phi_{u_0^{(1)}v_0^{(1)}}(0)}{\sqrt{\frac{E_1}{N_cN}\sum_{l=1}^{N_c} l\left[\phi_{u_0^{(1)}v_0^{(1)}}(-lT_c)+\phi_{u_0^{(1)}v_0^{(1)}}(lT_c)\right]^2+\frac{1}{N}\sum_{k=2}^{K}\sum_{l=-N_c}^{N_c-1}E_k\phi^2_{u_0^{(k)}v_0^{(1)}}(lT_c+\epsilon_k)+\sigma^2\phi_{v_0^{(1)}}(0)}}\right), \tag{35}$$

for large N_f/N_p, where $\boldsymbol{\epsilon} = [\epsilon_2 \cdots \epsilon_K]$ characterizes the asynchronism between the interfering users and the desired user in $modulo\ T_c$ arithmetic. Similar to the multi-pulse case, the unconditional BEP is given by $P_e^{\text{sync}} = P_e(\mathbf{0})$, with $P_e(\boldsymbol{\epsilon})$ being as in (35), for the synchronous case, and by

$$P_e^{\text{async}} \approx \frac{1}{T_c^{K-1}}\int_0^{T_c}\cdots\int_0^{T_c} P_e(\boldsymbol{\tau})d\tau_0^{(2)}\ldots d\tau_0^{(K)}, \tag{36}$$

for the asynchronous case.

From the closed-form BEP expressions for multi-pulse and single-pulse systems, we can observe that the IFI and MAI terms depend on the autocorrelation function of a single pulse for single-pulse systems, they depend also on the cross-correlations of different pulse types for multi-pulse systems, which suggests that more flexibility in combatting the effects of the IFI and MAI is present in multi-pulse systems. In other words, by design of UWB pulses with good cross-correlation properties, it is possible to mitigate the IFI and MAI to a larger extent, as will be investigated in Section VII.

VI. Multi-Pulse Transmitted Reference Impulse Radio Systems

TR-IR systems [7], [20]-[22] relax the stringent timing requirements of the SR-IR systems [2], and do not need any channel estimation, which is a challenging task for coherent UWB-IR receivers [23]. However, the main drawbacks of the original TR-IR proposal [7] are the use of energy for the reference pulses and the effects of using a noisy template signal which causes a large noise-noise term at the correlator output. In order to reduce the effects of the latter problem, the received signal can be passed through a matched filter [21], or an averaging operation can be performed [22]. In this section, we design a transmitter-receiver structure, which allows the use of different types of UWB pulses in the system, thus provides robustness against MAI and IFI. In order to reduce the effects of the noise-noise cross-terms, the approaches proposed in [21] and [22] can be straightforwardly applied to our multi-pulse receiver, which we do not consider in this paper, and mainly focus on mitigating the effects of IFI and MAI by means of multiple types of UWB pulses.

If we consider the "conventional" TR signalling structure as shown in Figure 3-(a), we observe that each reference pulse is followed by a data pulse after T_d seconds [7]. One way to adopt the use of multiple types of UWB pulses is to consider transmitting a sequence of reference and data pulses of the same type, as shown in Figure 3-(b). The same pulse types are considered for each reference and data pulse pair in order to facilitate a simple demodulation scheme (with delay-and-multiply operations) at the receiver side. Although the scheme in Figure 3-(b) is a simple way of implementing a multi-pulse TR system, it may not have enough rejection of reference-to-data interference under harsh multipath conditions since the same pulse type needs to be employed for each reference and data pulse pair[6]. Therefore, we propose the signalling scheme shown in Figure 1, where N_p reference pulses are transmitted first, followed by the corresponding N_p data pulses, and then the next N_p reference pulses and the corresponding N_p data pulses are transmitted, and this structure continues until a total of $N_f/2$ reference pulses and $N_f/2$ data

[6]The adverse effects of reference-to-data interference and IFI in TR-IR systems are investigated in [24].

pulses are transmitted. In this way, each pulse is followed by a different type of UWB pulse, and therefore the interference between consecutive pulses can be mitigated by appropriate choice of pulse structures.

For the signal model in Figure 1, which is described in Section II-B, we propose the receiver structure in Figure 4, which has N_p parallel branches, each of which processes one type of UWB pulse. In other words, the received signal is first passed through a bank of delay-and-multiply operators, each for a different pulse type. The output corresponding to the jth frame of the nth pulse type is given by

$$Y_{n,j} = \int_{T_{n,j}^{(1)}}^{T_{n,j}^{(1)}+T_{\text{int}}} r(t)r(t-T_n^{(1)})dt, \tag{37}$$

for $n = 0, 1, \ldots, N_p - 1$, and $j = 0, 1, \ldots, N_f/(2N_p) - 1$, where $T_{n,j}^{(k)} = (2jN_p + n)T_f + T_n^{(k)} + c_{2jN_p+n}^{(k)} T_c$, T_{int} is the integration interval, and the 0th bit of user 1 is considered without loss of generality. Then, at each branch, the contributions from different frames are combined; that is, $Y_n = \sum_{j=0}^{N_f/(2N_p)-1} Y_{n,j}$, for $n = 0, 1, \ldots, N_p - 1$. Note that we consider a general model in which the distance between the reference and data pulses can be different for different types of pulses and for different users.

After obtaining the decision variables at different branches, we can estimate the information bit as follows

$$\hat{b}_0 = \text{sign}\left\{ \sum_{n=0}^{N_p-1} w_n Y_n \right\}, \tag{38}$$

where $w_0, \ldots, w_{N_p-1}$ are the weighting coefficients at different branches. For example, if statistical information on $\{Y_n\}_{n=0}^{N_p-1}$ is available, the weights can be chosen according to the MMSE criterion. However, this is usually not possible unless the receiver can store $\{Y_n\}_{n=0}^{N_p-1}$ values for a number of information bits and the system is stable, meaning that the statistics of the total noise (MAI, IFI, and thermal noise) do not change during the reception of those information bits. Therefore, a practical choice is to use equal gain combining (EGC); that is, $w_0 = \cdots = w_{N_p-1} = 1$.

In the case of EGC, if we use the same delay between the reference and data pulses for all the pulses of user 1; that is, $T_n^{(1)} = T^{(1)}\ \forall n$, we can have a simpler receiver with a single delay-and-multiply operator, as shown in Figure 5.

The advantage of the multi-pulse TR system over a single-pulse TR system is that the former can provide better rejection of the MAI and the IFI, since different pulse shapes with good cross-correlation properties can be employed. If the main source of error is the thermal noise, then the two systems are expected to perform almost the same.

A. Approximate Performance Analysis

In this section, we present an approximate analysis of the proposed TR-IR receiver, based on a set of simplifying assumptions. The details of the derivations are omitted due to space limitations.

We first assume that $T_n^{(k)} = T^{(k)}\ \forall n$, and T_{int} is smaller than the maximum delay spread of the channel. Then, we also assume that there is no IFI in the system[7] by assuming a sufficiently large frame interval compared to the delay spread of the channel and constraining the TH sequences into the set $\{0, 1, \ldots, N_h - 1\}$, where $N_h T_c + \tau_{L-1}^{(1)} < T_f$.

We consider a MAI-limited scenario, in which the MAI is much stronger than the thermal noise. Note that the advantage of the multi-pulse system in mitigating the effects of the interference would be significant in this scenario. For a system with dominant thermal noise, the single- and multi-pulse systems are expected to perform the same. In the MAI-limited scenario, the output from the jth frame of the nth pulse given by (37) can be approximately expressed, using (8), as

$$Y_{n,j} = b_0^{(1)} \frac{E_1}{N_f} \int_0^{T_{\text{int}}} \left[u_n^{(1)}(t)\right]^2 dt + \eta_{n,j} + \zeta_{n,j}, \tag{39}$$

where $u_n^{(k)}(t)$ is given by (9), $\eta_{n,j}$ is the MAI-signal term, and $\zeta_{n,j}$ is the MAI-MAI term. The MAI-signal and MAI-MAI terms are given, respectively, by

$$\begin{aligned} \eta_{n,j} &= \sum_{k=2}^{K} \frac{\sqrt{E_1 E_k}}{N_f} \int_{T_{n,j}^{(1)}}^{T_{n,j}^{(1)}+T_{\text{int}}} \left[r^{(1)}(t) r^{(k)}(t - T_n^{(1)}) + r^{(k)}(t) r^{(1)}(t - T_n^{(1)})\right] dt, \\ \zeta_{n,j} &= \sum_{k_1=2}^{K} \sum_{k_2=2}^{K} \frac{\sqrt{E_{k_1} E_{k_2}}}{N_f} \int_{T_{n,j}^{(1)}}^{T_{n,j}^{(1)}+T_{\text{int}}} r^{(k_1)}(t) r^{(k_2)}(t - T_n^{(1)}) dt, \end{aligned} \tag{40}$$

where $r^{(k)}(t)$ is the part of the received signal related to user k:

$$r^{(k)}(t) = \sum_{i=-\infty}^{\infty} \sum_{n=0}^{N_p-1} \sum_{j=iN_f/(2N_p)}^{(i+1)\frac{N_f}{2N_p}-1} \left\{ d_{2jN_p+n}^{(k)}\, u_n^{(k)}\left(t - T_{n,j}^{(k)} + T_n^{(k)}\right) + b_{\lfloor 2jN_p/N_f \rfloor}^{(k)}\, d_{2jN_p+n}^{(k)}\, u_n^{(k)}\left(t - T_{n,j}^{(k)}\right) \right\}. \tag{41}$$

[7]Note that the better suppression of the IFI is in fact an advantage of the multi-pulse TR systems that we consider. The purpose of this simplified analysis is to present some initial results on the performance of our proposed receiver. A more detailed analysis is to be performed in a future study.

It can be shown that the noise terms, $\eta_{n,j}$ and $\zeta_{n,j}$, have zero mean, by using the fact that the polarity codes are i.i.d. for different users. From (39) and (40), it is straightforward but cumbersome to derive the signal-to-interference ratio (SIR) of the system, which results in a quite complex expression. However, under the condition that $|T^{(k)}-T^{(1)}| > \tau_{L-1}^{(k)} - \tau_0^{(k)} + T_c$ for $k = 2, \ldots, K$, the following relatively simpler expression for the SIR can be obtained after some manipulation:

$$\mathrm{SIR}(\boldsymbol{\tau}) = \frac{E_1^2 N_f^2 \left(\sum_{n=0}^{N_p-1} \int_0^{T_{\mathrm{int}}} \left[u_n^{(1)}(t) \right]^2 dt \right)^2}{4N_p^2 \sum_{n=0}^{N_p-1} \sum_{j=0}^{\frac{N_f}{2N_p}-1} \int_0^{T_{\mathrm{int}}} \int_0^{T_{\mathrm{int}}} \sigma_{n,j}^2(t_1, t_2; \boldsymbol{\tau}) dt_1 dt_2}, \tag{42}$$

where $\boldsymbol{\tau} = [\tau_0^{(2)} \cdots \tau_0^{(K)}]$ is the delay of the interfering users, and

$$\begin{aligned} \sigma_{n,j}^2(t_1, t_2; \boldsymbol{\tau}) = {} & E_1 u_n^{(1)}(t_1) u_n^{(1)}(t_2) \sum_{k=2}^{K} E_k \sum_{x \in \mathcal{B}} f_{n,j}^{(k)}(t_1, t_2; x + \tau_0^{(k)}) \\ & + \sum_{\substack{k_1=2 \\ k_1 \neq k_2}}^{K} \sum_{k_2=2}^{K} E_{k_1} E_{k_2} \sum_{(x,y) \in \mathcal{C}} h_{n,j}^{(k_1,k_2)}(t_1, t_2; x + \tau_0^{(k_1)}, y + \tau_0^{(k_2)}), \end{aligned} \tag{43}$$

with $\mathcal{B} = \{-T^{(1)}, 0, T^{(k)} - T^{(1)}, T^{(k)}\}$, $\mathcal{C} = \{(-T^{(1)}, 0), (-T^{(1)}, T^{(k_2)}), (T^{(k_1)} - T^{(1)}, 0), (T^{(k_1)} - T^{(1)}, T^{(k_2)})\}$,

$$f_{n,j}^{(k)}(t_1, t_2; x) = \frac{1}{N_h^2} \sum_{i=-\frac{N_f}{2N_p}}^{\frac{N_f}{2N_p}-1} \sum_{m=0}^{N_p-1} \sum_{l=-(N_h-1)}^{N_h-1} (N_h - |l|)\, u_m^{(k)}(t_1 + T_{j,i,n,m,l} - x)\, u_m^{(k)}(t_2 + T_{j,i,n,m,l} - x), \tag{44}$$

and

$$h_{n,j}^{(k_1,k_2)}(t_1, t_2; x, y) = \frac{1}{N_h^3} \sum_{\substack{l_1=-(N_h-1) \\ |l_1-l_2|<N_h}}^{N_h-1} \sum_{l_2=-(N_h-1)}^{N_h-1} (N_h - \gamma_{l_1,l_2})\, g_{n,j,l_1}^{(k_1)}(t_1, t_2; x)\, g_{n,j,l_2}^{(k_2)}(t_1, t_2; y). \tag{45}$$

In equation (45), $g_{n,j,l}^{(k)}(t_1, t_2; x)$ is given by

$$g_{n,j,l}^{(k)}(t_1, t_2; x) = \sum_{i=-\frac{N_f}{2N_p}}^{\frac{N_f}{2N_p}-1} \sum_{m=0}^{N_p-1} u_m^{(k)}(t_1 + T_{j,i,n,m,l} - x)\, u_m^{(k)}(t_2 + T_{j,i,n,m,l} - x), \tag{46}$$

with $T_{j,i,n,m,l} = (2N_p(j-i) + n - m)T_f + lT_c$, and γ_{l_1,l_2} is equal to $\max\{|l_1|, |l_2|\}$ if the signs of l_1 and l_2 are the same, and is equal to $|l_1| + |l_2|$ otherwise.

Note that even though the expressions seem complicated, the numerical evaluation of the SIR can be performed usually in a reasonable period of time using (42)-(46).

As considered in [31], if we approximate the sum of the noise terms by a Gaussian random variable for large numbers of users under the assumption of perfect power control, we can approximate the BEP of the system by $P_e(\boldsymbol{\tau}) \approx Q\left(\sqrt{\mathrm{SIR}(\boldsymbol{\tau})}\right)$. For an asynchronous system, the expectation over the interfering users' delays needs to be taken, which might be approximated by Monte-Carlo simulations.

VII. Simulation Results

In this section, we first compare the BEP performance of a single pulse and a double-pulse SR-IR system. In the double-pulse system, each user transmits the 4th and 5th order MHPs [11] alternately, whereas the single-pulse system employs the 4th order MHP in all the frames (see Figure 6). The systems parameters are $K = 5$ users, $N_f = 20$ frames per symbol, $N_c = 30$ chips per frame, and $T_c = 1$ ns. We consider an MAI-limited scenario, where the received energy of each interferer is 18.75dB more than that of the user of interest. All the channels have $L = 20$ taps, which are generated independently according to a channel model with exponentially decaying ($\mathrm{E}\{|\alpha_l|^2\} = \Omega_0 e^{-\lambda l}$) log-normal fading ($|\alpha_l| \sim \mathcal{LN}(\mu_l, \sigma^2)$) channel amplitudes, random signs for channel taps, and exponential distribution for the path arrivals with a mean $\hat{\mu}$. The channel parameters are $\lambda = 0.5$, $\sigma^2 = 1$, and $\hat{\mu} = 1.5$ ns, and μ_l can be calculated from $\mu_l = 0.5\left[\ln(\frac{1-e^{-\lambda}}{1-e^{-\lambda L}}) - \lambda l - 2\sigma^2\right]$, for $l = 0, 1, \ldots, L-1$.

Figure 7 shows the BEP performance of all-RAKE receivers [16] for the single and double-pulse systems. Both the theoretical and the simulation results are shown, which are in good agreement. From the figure, the double-pulse system is observed to have a better performance than the single-pulse system, as expected. Further gains can be obtained by using a larger number of UWB pulse types and/or MHPs that are several orders apart [11].

Next, we evaluate the accuracy of the approximate analysis in Section VI-A for a synchronous double-pulse TR-IR system. The parameters are given by $K = 10$ users, with $E_1 = 1$ and $E_k = E$ for $k = 2, \ldots, K$, $L = 5$ multipath components with the same channel model described previously, $T_c = 1$ ns, $N_c = 20$, $N_f = 4$, and $T_{\text{int}} = 1$ ns. In order to satisfy the assumptions of the analysis, $N_h = 3$, $T^{(1)} = 40$, and $T^{(k)} = 51$ for $k = 2, \ldots, K$ are used. The 4th and 5th order MHPs are employed alternatively, and the SIR of the system is plotted in Figure 8 for various E values. From the figure, a reasonably good match between the theory and the simulations is observed.

Finally, we perform a simulation study of the TR-IR system with more realistic parameters, where $K = 10$, $L = 10$, $T_c = 1$ ns, $N_f = 8$, $N_c = N_h = 20$, $T_{\text{int}} = 6$ ns, $E_1 = 1$ and $E_k = 0.5$ for $k = 2, \ldots, K$

are used. An asynchronous system is assumed, and both a single-pulse and a double-pulse system is considered as in the SR-IR simulations. The delays between the reference and the data pulses are set according to $T^{(k)} = N_p N_c \ \forall k$, where N_p is the number of pulse types. Figure 9 plots the BEPs of the single- and double-pulse systems for various noise levels. From the figure, it is observed that when the MAI is dominant, the double-pulse system performs better than the single-pulse system as expected.

VIII. Conclusions

In this paper, we have considered multi-pulse IR systems. First, we have introduced a generic model for an IR signal, which can represent an SR or a TR signal as special cases. Using this model, we have investigated the average PSD of the transmitted signal, which is important considering the power limitations imposed by the FCC. Then, we have provided a detailed BEP analysis for a multi-pulse SR-IR system, considering the effects of both the IFI and the MAI. In addition, we have proposed a multi-pulse scheme for TR-IR systems, in which a parallel or serial receiver implementation is possible. An approximate analysis of the TR-IR system has been presented, and simulations have verified its accuracy.

Appendix

A. Derivation of $\mathrm{E}\{s_{i,n}(t+\tau)s_{i,n}(t)\}$

Consider the expression in (2). Note that for both the SR and the TR system, the polarity codes are independent for different values of the index of the summation, j. Therefore, $\mathrm{E}\{s_{i,n}(t+\tau)s_{i,n}(t)\}$ is given by

$$\mathrm{E}\{s_{i,n}(t+\tau)s_{i,n}(t)\} = \sum_{j=iN_f/(2N_p)}^{(i+1)N_f/(2N_p)-1} \mathrm{E}\{\, p_n\left(t+\tau-(2jN_p+n)T_f - c_{2jN_p+n}T_c\right) p_n\left(t-(2jN_p+n)T_f - c_{2jN_p+n}T_c\right)$$
$$+ b_{1,j}\, b_{2,j}\, d_{2jN_p+n}\, d_{(2j+1)N_p+n}\, p_n\left(t+\tau-(2jN_p+n)T_f - c_{2jN_p+n}T_c\right) p_n\left(t-((2j+1)N_p+n)T_f - c_{(2j+1)N_p+n}T_c\right)$$
$$+ b_{1,j}\, b_{2,j}\, d_{2jN_p+n}\, d_{(2j+1)N_p+n}\, p_n\left(t+\tau-((2j+1)N_p+n)T_f - c_{(2j+1)N_p+n}T_c\right) p_n\left(t-(2jN_p+n)T_f - c_{2jN_p+n}T_c\right)$$
$$+ p_n\left(t+\tau-((2j+1)N_p+n)T_f - c_{(2j+1)N_p+n}T_c\right) p_n\left(t-((2j+1)N_p+n)T_f - c_{(2j+1)N_p+n}T_c\right) \}. \tag{47}$$

For the IR system, $b_{1,j} = b_{2,j} \in \{-1,+1\}$ and d_{2jN_p+n} and $d_{(2j+1)N_p+n}$ are independent, and thus the second and the third terms become zero after the expectation. For the TR system $b_{1,j} = 1$, $b_{2,j} \in \{-1,+1\}$, and $d_{2jN_p+n} = d_{(2j+1)N_p+n}$. So, the second and the third terms become independent for equiprobable information bits. Therefore, (47) can be expressed as

$$\sum_{j=iN_f/N_p}^{(i+1)N_f/N_p-1} \mathrm{E}\{p_n\left(t+\tau-(jN_p+n)T_f-c_{jN_p+n}T_c\right)p_n\left(t-(jN_p+n)T_f-c_{jN_p+n}T_c\right)\}, \tag{48}$$

after arranging the indices.

B. Proof of Proposition 5.1

Consider the IFI term given by (18); that is, $I=\sqrt{\frac{E_1}{N_r}}\sum_{j=0}^{N_r-1}\tilde{I}_j$, with $\tilde{I}_j=\frac{1}{\sqrt{N_p}}\sum_{n=0}^{N_p-1}\hat{I}_{jN_p+n}$. From (17), it can be shown that $\mathrm{E}\{\tilde{I}_j\}=0$, $\forall j$ due to the i.i.d. random polarity codes. Also from the $N_p\geq 2$ assumption in the proposition, it is straightforward to show, from (17), that $\mathrm{E}\{\tilde{I}_j\tilde{I}_{j+l}\}=0$ for $l\geq 2$, since $\tilde{I}_j$ and $\tilde{I}_{j+l}$ include terms with polarity codes of different indices, which are independent and zero mean by assumption. Hence, $\{\tilde{I}_j\}_{j=0}^{N_r-1}$ forms a zero mean 1-dependent sequence.

We employ the following central limit argument for dependent sequences in order to approximate the distribution of the IFI:

Theorem 1: [30] Consider a stationary d-dependent sequence of random variables $X_1, X_2, ...$ with $\mathrm{E}\{X_1\}=0$ and $\mathrm{E}\{|X_1|^3\}<\infty$. If $S_n=X_1+\ldots+X_n$, then $\frac{S_n}{\sqrt{n}}\longrightarrow\mathcal{N}(0,\sigma^2)$, *as* $n\longrightarrow\infty$, *where* $\sigma^2=\mathrm{E}\{X_1^2\}+2\sum_{k=1}^{d}\mathrm{E}\{X_1X_{1+k}\}$.

In order to apply the results of the theorem we first calculate the variance of $\tilde{I}_j$:

$$\mathrm{E}\{\tilde{I}_j^2\}=\frac{1}{N_p}\sum_{n_1=0}^{N_p-1}\sum_{n_2=0}^{N_p-1}\mathrm{E}\{\hat{I}_{jN_p+n_1}\hat{I}_{jN_p+n_2}\} \tag{49}$$

$$=\frac{1}{N_p}\sum_{n=0}^{N_p-1}\mathrm{E}\{\hat{I}_{jN_p+n}^2\}+\sum_{|n_1-n_2|=1}\mathrm{E}\{\hat{I}_{jN_p+n_1}\hat{I}_{jN_p+n_2}\}, \tag{50}$$

where the second equality is obtained from (17) by using the fact that the polarity codes form an i.i.d. sequence. Then, after some manipulation, $\mathrm{E}\{\hat{I}_j^2\}$ can be expressed as

$$\mathrm{E}\{\hat{I}_j^2\}=\frac{1}{N_c^2}\sum_{l=1}^{N_c}l\left[\phi^2_{u_{j-1}^{(1)}v_j^{(1)}}(-lT_c)+\phi^2_{u_{j+1}^{(1)}v_j^{(1)}}(lT_c)\right], \tag{51}$$

and $\mathrm{E}\{\hat{I}_j\hat{I}_{j+1}\}$ can be expressed as

$$\mathrm{E}\{\hat{I}_j\hat{I}_{j+1}\}=\frac{1}{N_c^2}\sum_{l=1}^{N_c}l\phi_{u_{j+1}^{(1)}v_j^{(1)}}(lT_c)\phi_{u_j^{(1)}v_{j+1}^{(1)}}(-lT_c). \tag{52}$$

In obtaining (51) and (52), we have used the expression in (17) and the facts that the polarity codes are randomly distributed in $\{-1,+1\}$ and the TH codes in $\{0,1,\ldots,N_c-1\}$.

Now considering the correlation between the adjacent terms of $\{\tilde{I}_j\}_{j=0}^{N_r-1}$, the following expression can be obtained:

$$\mathrm{E}\{\tilde{I}_j\tilde{I}_{j+1}\} = \frac{1}{N_p}\mathrm{E}\{\hat{I}_{(j+1)N_p-1}\hat{I}_{(j+1)N_p}\}. \tag{53}$$

Theorem 1 can be invoked for $\{\tilde{I}_j\}_{j=0}^{N_r-1}$, which results in $I\sim\mathcal{N}\left(0\,,\,E_1[\mathrm{E}\{\tilde{I}_j^2\}+2\mathrm{E}\{\tilde{I}_j\tilde{I}_{j+1}\}]\right)$. Then, from (49)-(53), the distribution of I can be approximated as

$$I\sim\mathcal{N}\left(0\,,\,\frac{E_1}{N_pN_c^2}\sum_{n=0}^{N_p-1}\left[\sigma^2_{\mathrm{IFI},1}(n)+2\sigma^2_{\mathrm{IFI},2}(n)\right]\right), \tag{54}$$

as $N_r\longrightarrow\infty$, where $\sigma^2_{\mathrm{IFI},1}(n)$ and $\sigma^2_{\mathrm{IFI},2}(n)$ are as in (20) and (21), respectively.

C. Proof of Proposition 5.2

Since $N_f=N_rN_p$, the MAI term given by (25) can be expressed as $M^{(k)}=\sqrt{\frac{E_k}{N_r}}\sum_{j=0}^{N_r-1}\tilde{M}_j^{(k)}$, where $\tilde{M}_j^{(k)}=\frac{1}{\sqrt{N_p}}\sum_{n=0}^{N_p-1}\hat{M}^{(k)}_{jN_p+n}$, with $\hat{M}_j^{(k)}$ being given by (26). Consider the sequence $\{\tilde{M}_j^{(k)}\}_{j=0}^{N_r-1}$. Since we assume that the delay spread of the channel is smaller than a frame interval, it can be shown that the elements of this sequence form a 3-dependent sequence for $N_p=1$, a 2-dependent sequence for $N_p=2$, and a 1-dependent sequence for $N_p\geq 3$. In any case, the distribution of $M^{(k)}$, given the delay of user k, converges to the following distribution by the central limit argument for dependent sequences in Appendix B:

$$M^{(k)}|\tau_0^{(k)}\sim\mathcal{N}\left(0\,,\,E_k\mathrm{E}\{(\tilde{M}_j^{(k)})^2|\tau_0^{(k)}\}\right), \tag{55}$$

as $N_r\longrightarrow\infty$, since $\mathrm{E}\{\tilde{M}_j^{(k)}|\tau_0^{(k)}\}=0$ and $\mathrm{E}\{\tilde{M}_{j_1}^{(k)}\tilde{M}_{j_2}^{(k)}|\tau_0^{(k)}\}=0$ for $j_1\neq j_2$ due the i.i.d. random polarity codes.

Also $\mathrm{E}\{(\tilde{M}_j^{(k)})^2|\tau_0^{(k)}\}$ can be calculated from $\tilde{M}_j^{(k)}=\frac{1}{\sqrt{N_p}}\sum_{n=0}^{N_p-1}\hat{M}^{(k)}_{jN_p+n}$ and (26), after some manipulation, as

$$\mathrm{E}\{(\tilde{M}_j^{(k)})^2|\tau_0^{(k)}\}=\frac{1}{N_p}\sum_{n=0}^{N_p-1}\mathrm{E}\{(\hat{M}^{(k)}_{jN_p+n})^2|\tau_0^{(k)}\}, \tag{56}$$

with

$$\mathrm{E}\{(\hat{M}_n^{(k)})^2|\tau_0^{(k)}\} = \frac{1}{N_c^2} \sum_{m=\left\lceil n-2+\frac{1}{N_c}-\frac{\tau_0^{(k)}}{T_f} \right\rceil}^{\left\lfloor n+2-\frac{1}{N_c}-\frac{\tau_0^{(k)}}{T_f} \right\rfloor} \sum_{l=-(N_c-1)}^{N_c-1} (N_c-|l|)\phi^2_{u_m^{(k)}v_n^{(1)}}\left(((m-n)N_c+l)T_c+\tau_0^{(k)}\right), \quad (57)$$

where the uniform distribution of i.i.d. TH sequences in $\{0,1,\ldots,N_c-1\}$ and i.i.d. random polarity codes are employed. Note that the limits of the first summation in (57) is determined by the fact that $\phi_{u_m^{(k)}v_n^{(l)}}(x)=0$ for $|x|>N_cT_c$.

From (55)-(57), the distribution of $M^{(k)}$, conditioned on the delay of user k, is obtained as in Proposition 5.2.

REFERENCES

[1] U. S. Federal Communications Commission, FCC 02-48: First Report and Order.

[2] M. Z. Win and R. A. Scholtz, “Impulse radio: How it works,” *IEEE Communications Letters,* vol. 2, no. 2, pp. 36-38, Feb. 1998.

[3] M. Z. Win and R. A. Scholtz, “Ultra-wide bandwidth time-hopping spread-spectrum impulse radio for wireless multiple-access communications,” *IEEE Transactions on Communications*, vol. 48, pp. 679-691, April 2000.

[4] F. Ramirez Mireless, “On the performance of ultra-wideband signals in Gaussian noise and dense multipath,” *IEEE Transactions on Vehicular Technology,* vol. 50, no.1, pp. 244-249, Jan. 2001.

[5] R. A. Scholtz, “Multiple access with time-hopping impulse modulation,” *Proc. IEEE Military Communications Conference (MILCOM 1993),* vol. 2, pp. 447-450, Boston, MA, Oct. 1993.

[6] D. Cassioli, M. Z. Win and A. F. Molisch, “The ultra-wide bandwidth indoor channel: From statistical model to simulations,” *IEEE Journal on Selected Areas in Communications*, vol. 20, pp. 1247-1257, Aug. 2002.

[7] R. Hoctor and H. Tomlinson, “Delay-hopped transmitted-reference RF communications,” *Proceedings of the IEEE Conference of Ultra Wideband Systems and Technologies 2002 (UWBST’02),* pp. 265-269, Baltimore, MD, May 2002.

[8] M.-H. Chung and R. A. Scholtz, “Comparison of transmitted- and stored-reference systems for ultra-wideband communications,” *Proc. IEEE Military Communications Conference (MILCOM 2004),* Monterey, CA, Oct. 31-Nov. 3, 2004.

[9] S. Gezici, H. Kobayashi, H. V. Poor and A. F. Molisch, “Performance evaluation of impulse radio UWB systems with pulse-based polarity randomization in asynchronous multiuser environments,” *Proc. IEEE Wireless Communications and Networking Conference (WCNC 2004),* vol. 2, pp. 908-913, Atlanta, GA, March 21-25, 2004.

[10] S. Gezici, H. Kobayashi, H. V. Poor and A. F. Molisch, “The trade-off between processing gains of an impulse radio system in the presence of timing jitter,” *Proc. IEEE International Conference on Communications (ICC 2004),* vol. 6, pp. 3596-3600, Paris, France, June 20-24, 2004.

[11] H. Harada, K. Ikemoto and R. Kohno, “Modulation and hopping using modified Hermite pulses for UWB communications,” *Proc. IEEE Conference of Ultra Wideband Systems and Technologies (UWBST 2004),* pp. 336-340, Kyoto, Japan, May 2004.

[12] Y.-P. Nakache and A. F. Molisch, “Spectral shape of UWB signals - Influence of modulation format, multiple access scheme and pulse shape,” *Proceedings of the IEEE Vehicular Technology Conference, (VTC 2003-Spring)*, vol. 4, pp. 2510-2514, Jeju, Korea, April 2003.

[13] E. Fishler and H. V. Poor, “On the tradeoff between two types of processing gain,” *IEEE Transactions on Communications,* to appear .

[14] J. G. Proakis, *Digital Communications,* Mc Graw Hill, New York, 4th edition, 2000.

[15] N. Lehmann and A. M. Haimovich, “New approach to control the power spectral density of a time hopping UWB signal,” *Proc. the 37th Conference on Information Sciences and Systems (CISS03),* Baltimore, MD, March 2003.

[16] D. Cassioli, M. Z. Win, F. Vatalaro and A. F. Molisch, “Performance of low-complexity RAKE reception in a realistic UWB channel,” *Proceedings of the IEEE International Conference on Communications, 2002 (ICC 2002),* vol. 2, pp. 763-767, New York, NY, April 28-May 2, 2002.

[17] S. Gezici, A. F. Molisch, H. V. Poor, and H. Kobayashi, “The trade-off between processing gains of an impulse radio UWB system in the presence of timing jitter,” submitted to *IEEE Transactions on Communications,* July 2004.

[18] L. B. Michael, M. Ghavami, and R. Kohno, “Multiple pulse generator for ultra-wideband communication using Hermite polynomial based orthogonal pulses,” *Proc. IEEE Conference on Ultra Wideband Systems and Technologies (UWBST 2002),* pp. 47-51, Baltimore, MD, May 21-23, 2002.

[19] R. K. Morrow, Jr. and J. S. Lehnert, “Bit-to-bit error dependence in slotted DS/SSMA packet systems with random signature sequences,” *IEEE Transactions on Communications,* vol. 37, pp. 1052-1061, Oct. 1989.

[20] N. v. Stralen, A. Dentinger, K. Welles II,R. Gaus, R. Hoctor, and H. Tomlinson, “Delay hopped transmitted reference experimental results,” *Proceedings of the IEEE Conference of Ultra Wideband Systems and Technologies 2002 (UWBST’02),* pp. 93-98, Baltimore, MD, May 2002.

[21] F. Tufvesson and A. F. Molisch, “Ultra-wideband communication using hybrid matched filter correlation receivers,” *Proc. IEEE Vehicular Technology Conference (VTC 2004 Spring),* Milan, Italy, May 17-19, 2004.

[22] J. D. Choi and W. E. Stark, “Performance of ultra-wideband communications with suboptimal receivers in multipath channels,” *IEEE Journal on Selected Areas in Communications,* vol. 20, issue 9, pp. 1754-1766, Dec. 2002.

[23] V. Lottici, A. DÁndrea, and U. Mengali, “Channel estimation for ultra-wideband communications,” *IEEE Journal on Selected Areas in Communications,* vol. 20, issue 9, pp. 1638-1645, Dec. 2002.

[24] S. Gezici, F. Tufvesson and A. F. Molisch, “On the performance of transmitted-reference impulse radio,” *IEEE Global Telecommunications Conference (Globecom 2004),* pp. 2874-2879, Dallas, TX, Nov. 29-Dec. 3, 2004.

[25] P. Billingsley, *Probability and Measure,* John Wiley & Sons, New York, 2nd edition, 1986.

[26] FCC 00-163: Notice of Proposed Rule Making.

[27] M. B. Pursley, “Performance evaluation for phase-coded spread-spectrum multiple-access communication - Part I: System analysis,” *IEEE Transactions on Communications,* vol. COM-25, pp. 795799, Aug. 1977.

[28] D. E. Borth and M. B. Pursley, “Analysis of direct-sequence spread spectrum multiple-access communication over Rician fading channels,” *IEEE Transactions on Communications,* vol. COM-27, pp. 15661577, Oct. 1979.

[29] C. S. Gardner and J. A. Orr, “Fading effects on the performance of a spread spectrum multiple-access communication system,” *IEEE Transactions on Communications,* vol. COM-27, pp. 143149, Jan. 1979.

[30] W. Hoeffding and H. Robbins, “The central limit theorem for dependent random variables,” *J. Duke Math.,* 15, pp. 773780, 1948.

[31] L.-Y. Chao and R. A. Scholtz, “Multiple access performance of ultra-wideband transmitted reference systems in multipath environments,” *Proc. IEEE Wireless Communications and Networking Conference (WCNC 2004),* vol. 3, pp. 1788-1793, Atlanta, GA, March 21-25, 2004.

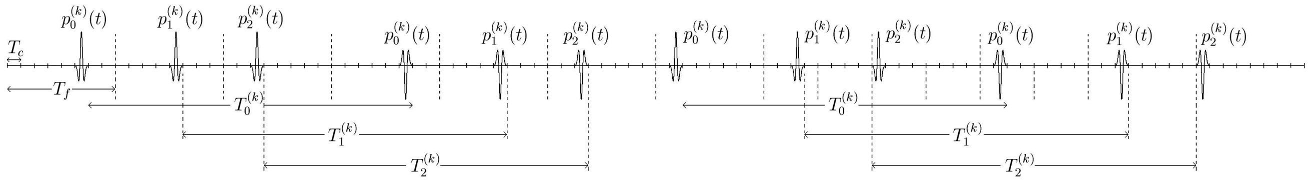

Fig. 1. Transmitted signal from a multi-pulse TR-IR system, where $N_f = 12$, $N_c = 8$, $T_n^{(k)} = \Delta T_c$ for $n = 0, 1, 2$ with $\Delta = 24$, and the TH sequence is $\{5, 4, 2, 5, 4, 2, 1, 2, 0, 1, 2, 0\}$. For simplicity, no polarity codes are shown (that is, $d_j^{(k)} = 1\ \forall j$), and $b_{1,j}^{(k)} = 1$ and $b_{2,j}^{(k)} = -1$.

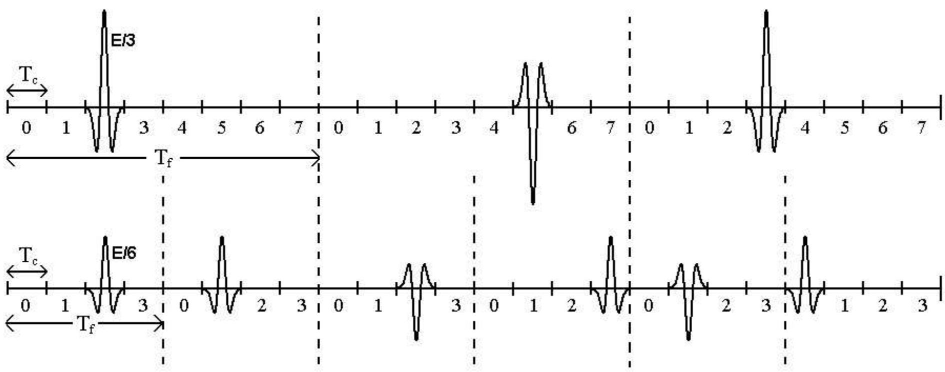

Fig. 2. Two different cases for an SR-IR system when $N_c N_f = 24$. For the first case, $N_c = 8$, $N_f = 3$ and the pulse energy is $E/3$; for the second case, $N_c = 4$, $N_f = 6$ and the pulse energy is $E/6$.

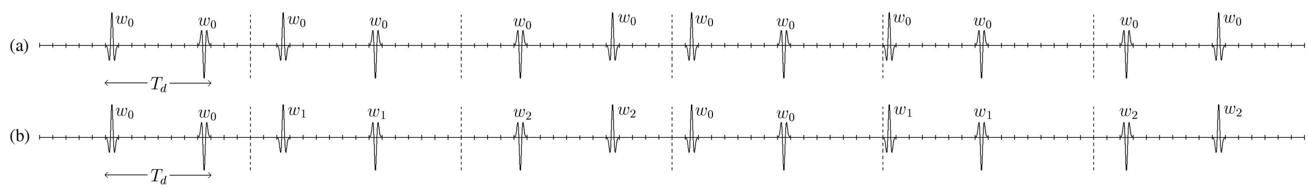

Fig. 3. (a) Transmitted signal from a conventional single-pulse TR-IR system. (b) An approach to employ multiple types of UWB pulses in a TR-IR system.

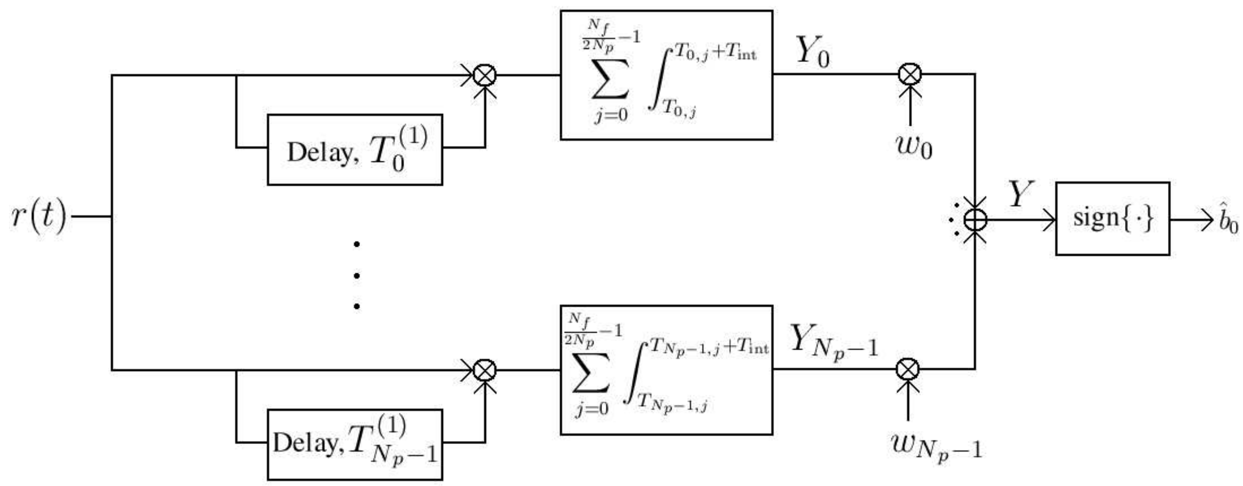

Fig. 4. The proposed receiver structure for the multi-pulse TR-IR system.

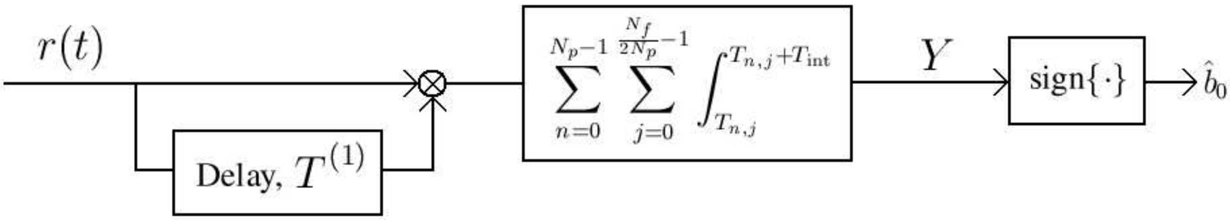

Fig. 5. The receiver structure for the multi-pulse TR-IR system when the same delay for all the pulses of user 1, and EGC are used.

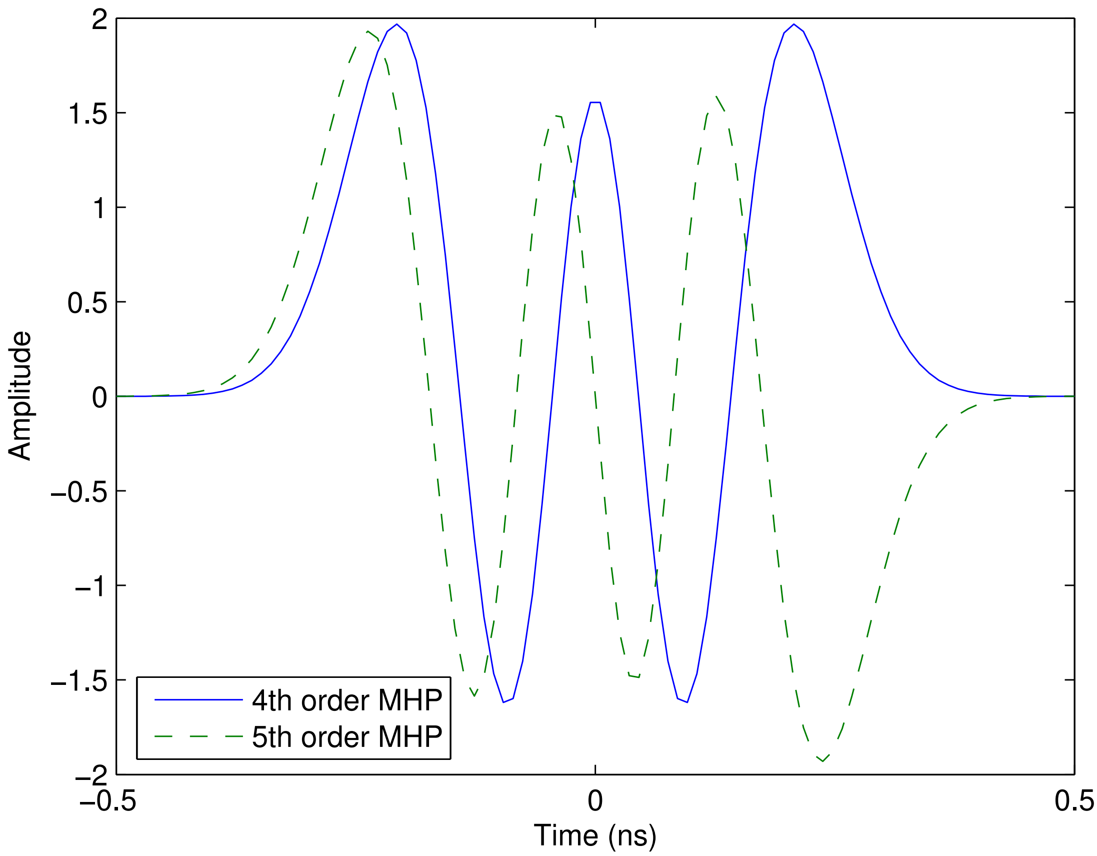

Fig. 6. The 4th and 5th order modified Hermite pulses (MHPs).

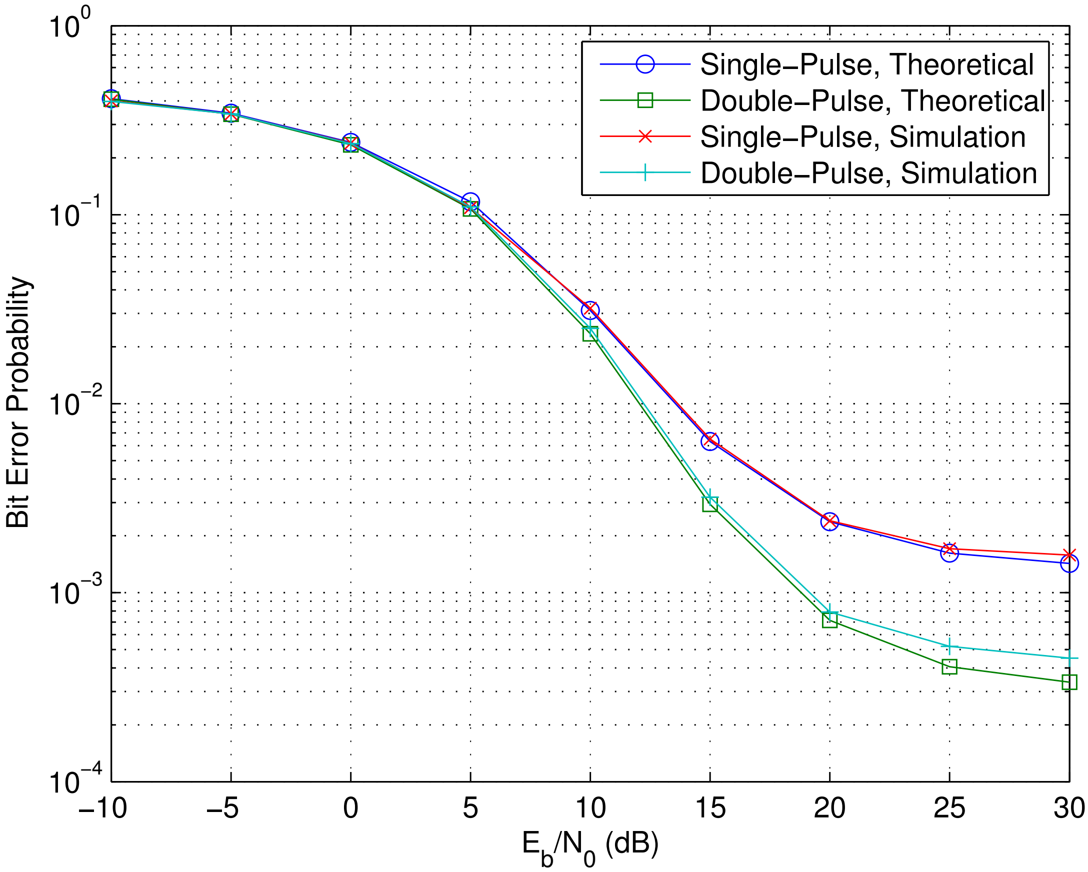

Fig. 7. The BEP performance of the single- and the double-pulse SR-IR systems.

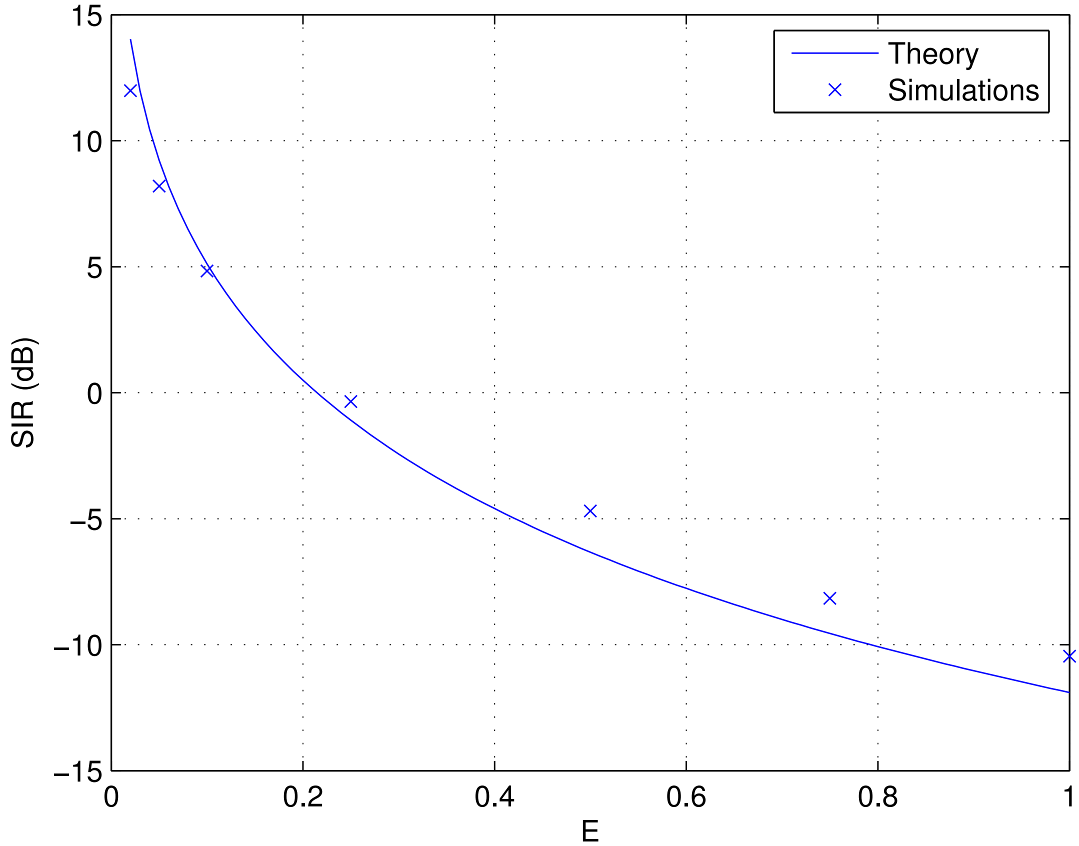

Fig. 8. The SIR values for a double-pulse TR-IR system for various energy levels of the interfering users.

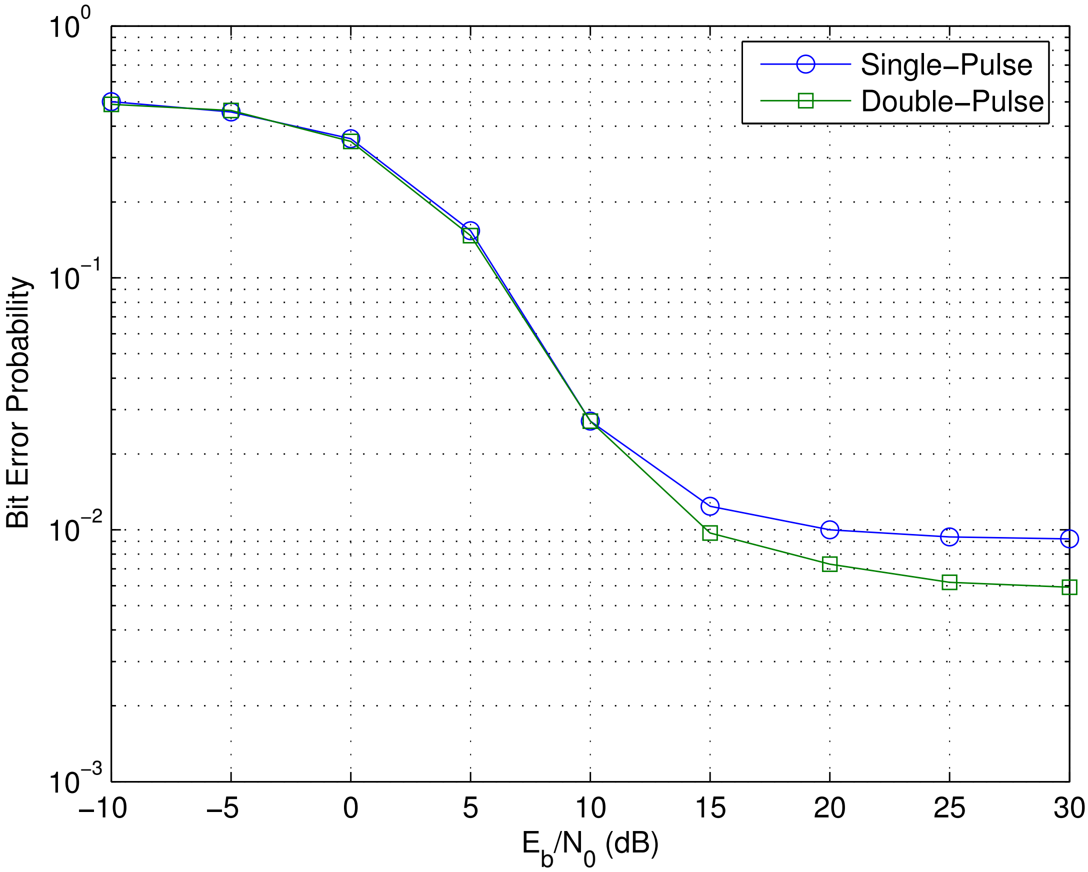

Fig. 9. The BEP performance of the single- and the double-pulse TR-IR systems.